

Double folding analysis of ^3He elastic and inelastic scattering to low lying states on ^{90}Zr , ^{116}Sn and ^{208}Pb at 270 MeV

Marwa N. El-Hammamy¹⁾

Physics Department, Faculty of Science, Damanhur University, Egypt

Abstract: The experimental data on elastic and inelastic scattering of 270 MeV ^3He particles to several low lying states in ^{90}Zr , ^{116}Sn and ^{208}Pb are analyzed within the double folding model (DFM). Fermi density distribution (FDD) of target nuclei is used to obtain real potentials with different powers. DF results are introduced into a modified DWUCK4 code to calculate the elastic and inelastic scattering cross sections. Two choices of potentials form factors are used; Woods Saxon (WS) and Woods Saxon Squared (WS^2) for real potential, while the imaginary part is taken as phenomenological Woods Saxon (PWS) and phenomenological Woods Saxon Squared (PWS^2). This comparison provides information about the similarities and differences of the models used in calculations.

Key words: elastic and inelastic scattering, double folding, squared fermi density distribution, Woods Saxon Squared potential, modified DWUCK4

PACS: 25.55.Ci **DOI:** 10.1088/1674-1137/39/3/034101

1 Introduction

When we bombard a nucleus with a nucleon or with light ions like d, ^3He , α -particles, etc., various nuclear phenomena occur, including elastic scattering, inelastic scattering, nucleon transfer reactions and projectile fragmentation, depending on the projectile species and the bombarding energy. The simplest among these phenomena is the elastic scattering. Elastic scattering can provide valuable information about the interaction potential between two colliding nuclei [1]. Inelastic scattering of ^3He particles provides useful methods for investigation of excited states of nuclei. According to the importance of these reactions, the analysis of experimental data on elastic and inelastic scattering of ^3He from different targets is needed [2–4]. The main problem with investigating the light heavy ion reactions by using nuclear reaction models is to determine the most suitable potential form to explain the experimental data. Optical (OM) and Folding models (FM) are examples of simplified models that exist for studying light heavy ion reactions [1, 5–8]. The OM has a potential including real and imaginary potentials. The real potential plays an important role in describing the elastic scattering of the reaction. The imaginary potential expresses the loss of flux into non elastic channels. The real and imaginary potentials can be determined with either the phenomenological or the microscopic model.

In the microscopic model, while the imaginary poten-

tial is taken as phenomenological Woods Saxon (PWS) or PWS^2 type potential, the real potential can be defined using the double folding model (DFM). In DFM, the density distributions (DD) of both projectile and target nuclei are used. Therefore, DD used in double folding calculations is very important in examining nuclear reactions.

The purpose of this work is to analyze angular distributions of the elastic and inelastic scattering of ^3He with an energy of 270 MeV leading to the excitation of ^{90}Zr levels, 2.18 MeV (2^+), 2.75 MeV (3^-), ^{116}Sn levels 1.29 MeV (2^+), 2.27 MeV (3^-), and ^{208}Pb levels 4.09 MeV (2^+), 2.61 MeV (3^-) MeV [2] in the framework of DFM by using Fermi density distribution (FDD) of target nuclei and Woods Saxon (WS) potential forms with different powers ($n=1$ or 2) as case one and case two. The similarities and differences between these two cases are pleasantly visible in this comparison. The importance of inelastic scattering analysis to low lying states is to test the strength of these states within DFM.

The method employed here and discussions are given in Section 2, and the conclusions are presented in Section 3.

2 Analysis and discussion

To study the elastic scattering for the reactions of ^3He - particles with ^{90}Zr , ^{116}Sn and ^{208}Pb , the program code DF POT [9] has been used. $V(r)$ is the DF potential

Received 5 June 2014

1) E-mail: marwa1374@yahoo.com

©2015 Chinese Physical Society and the Institute of High Energy Physics of the Chinese Academy of Sciences and the Institute of Modern Physics of the Chinese Academy of Sciences and IOP Publishing Ltd

carried out by introducing the effective nucleon-nucleon (NN) interaction over the ground state DD of the two colliding nuclei. It is evaluated from the expression

$$V(r) = \iint \rho_1(r_1) \rho_2(r_2) V_{NN}(s) dr_1 dr_2. \quad (1)$$

$\rho_1(r_1)$ and $\rho_2(r_2)$ are the nuclear matter density of the two colliding nuclei, and $V_{NN}(s)$ is the effective NN interaction potential ($s=r-r_2+r_1$). $V_{NN}(s)$ is taken to be a standard Reid-M3Y interaction [10] in the form,

$$V_{NN}(r) = 7999.0 \frac{e^{-4.0r}}{4.0r} - 2134.0 \frac{e^{-2.5r}}{2.5r} + J_{00}(E) \delta(r). \quad (2)$$

The first and second terms represent the direct part and the third term represents the exchange part of the interaction potential. It plays an important role in reproducing the experimental results for elastic and inelastic scattering [11, 12]. The exchange part can be written to a good approximation in the form [10]

$$J_{00}(E) = -276 \left(1 - 0.005 \frac{E}{A} \right), \quad (3)$$

where E is the energy in the center of mass system and A is the mass number of the projectile.

In our calculations, the nuclear matter DD of ${}^3\text{He}$ nucleus has the Gaussian form

$$\rho = \rho_0 \exp(-\alpha r^2), \quad (4)$$

where $\alpha = 0.5505 \text{ fm}^{-2}$, $\rho_0 = 0.2201 \text{ fm}^{-3}$ [13], and for ${}^{90}\text{Zr}$ [14], ${}^{116}\text{Sn}$ and ${}^{208}\text{Pb}$ [15] the following FDD form is used

$$\rho = \rho_0 \left[1 + \exp\left(\frac{r-R}{a}\right) \right]^{-n} \cdot (n=1 \text{ or } 2). \quad (5)$$

The total potential must comprise both the real part and the imaginary part, the latter being responsible for the absorption of the incident particle in the inelastic channels. Since the M3Y interaction is real, the folding calculation gives the real part of the potential.

$$U(r) = N_r V(r) + iW(r). \quad (6)$$

In the model used here, the volume real part has the folded form with normalization factors N_r . We have chosen this form to be WS shape, while the imaginary part is taken as PWS. The resulting folded form factors, in

addition with PWS potentials parameters in each case ($n=1$ or 2) are introduced into the modified program code DWUCK4 [16] to compute the differential scattering cross section, in which an additional form factor form WS^2 is added. The calculations for elastic scattering were calculated by DWUCK4. First, we used WS for real and PWS for imaginary parts of the potential as case one. Secondly, in case two, we used WS^2 for real and PWS^2 for imaginary parts of the potential. Thus, the real potentials are represented by

$$V(r) = -V_0 \left[1 + \exp\left(\frac{r-R_v}{a_v}\right) \right]^{-n},$$

while the imaginary potentials are represented by

$$W(r) = -W_0 \left[1 + \exp\left(\frac{r-R_w}{a_w}\right) \right]^{-n} \quad (7)$$

in which $R_{v,w} = r_{v,w} (A_T^{1/3} + A_P^{1/3})$ and $n=1$ or 2 . $V(r)$ is the DF potential of Eq. (1) and N_r , W_0 , r_w , a_w , are variable parameters. Comparisons are shown in Fig. 1 between the present calculations and experimental data.

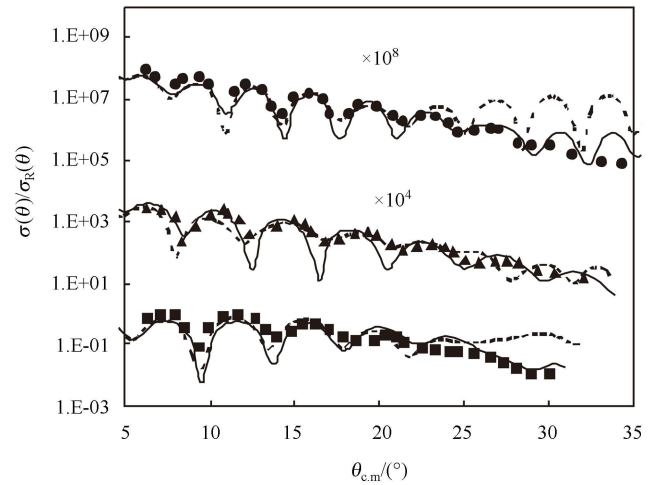


Fig. 1. Angular distributions of ${}^3\text{He}$ elastically scattered on ${}^{90}\text{Zr}$, ${}^{116}\text{Sn}$ and ${}^{208}\text{Pb}$. The theoretical cross section obtained with the DF model is represented by dotted lines for case one and solid lines for case two. Experimental points are denoted by black symbols, \blacksquare for ${}^{90}\text{Zr}$, \blacktriangle for ${}^{116}\text{Sn}$ and \bullet for ${}^{208}\text{Pb}$.

Table 1. The real and imaginary potentials parameters of ${}^3\text{He}$ elastic scattering on different nuclei.

reaction	n	V_0/MeV	R_v/fm	a_v/fm	N_r	W_0/MeV	r_w/fm	a_w/fm	χ_R^2
${}^3\text{He}+{}^{90}\text{Zr}$	1	143	4.292	1.228	0.78	20	1.20	0.24	0.19
	2	209	5.011	1.528	1	29	1.20	0.54	0.09
${}^3\text{He}+{}^{116}\text{Sn}$	1	143.4	4.795	1.238	0.69	20	1.14	1.0	0.11
	2	205.3	5.517	1.529	1	52	1.14	1.19	0.10
${}^3\text{He}+{}^{208}\text{Pb}$	1	143.8	6.136	1.222	0.69	20	1.18	0.24	0.31
	2	192.3	6.861	1.486	1	35	1.18	0.66	0.15

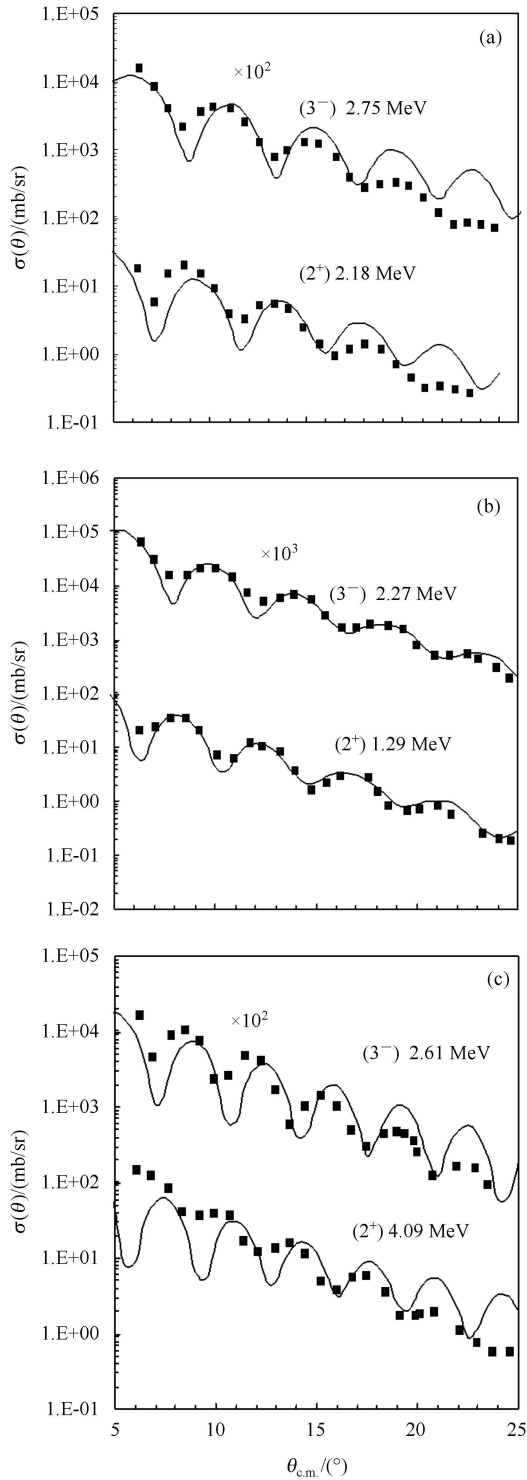


Fig. 2. Angular distributions of ${}^3\text{He}$ inelastically scattered on ${}^{90}\text{Zr}$ (a), ${}^{116}\text{Sn}$ (b) and ${}^{208}\text{Pb}$ (c). The theoretical cross section obtained with the DF model is represented by solid lines for case two. Experimental points are denoted by black symbols.

The variable parameters of the two cases and DF-equivalent potential parameters (V_0 , r_v , a_v) are listed in

Table 1. In order to estimate the quality of the fit, one can calculate a relative error

$$\chi_R^2 = \frac{1}{N} \sum_{i=1}^N \left[\frac{(\sigma^{\text{calc.}}(\theta_i) - \sigma^{\text{exp.}}(\theta_i))^2}{(\sigma^{\text{calc.}}(\theta_i) + \sigma^{\text{exp.}}(\theta_i))} \right], \quad (8)$$

where N is the number of data points and $\sigma^{\text{calc.}}(\theta_i)$ is the i^{th} calculated scattering cross section and $\sigma^{\text{exp.}}(\theta_i)$ is the corresponding experimental scattering cross section.

For the first case, the agreement of the theoretical angular distribution with the experimental one is excellent at forward angles $\theta_{\text{c.m.}} < 22^\circ$, then discrepancy appeared in larger angular regions. Thus, these results should be improved with another theoretical approach. Therefore secondly in case two, we increased the power of the potential form to be squared as it was successful in many other analyses within OM [17, 18]. According to an increase of the real normalization factor ($N_r = 1$) values by increasing power (n), the results are better than in case one, with less relative error χ_R^2 values. This is an important point in the study of the interaction of ${}^3\text{He}$ because, when investigated, the interaction of ${}^3\text{He}$ with different target nuclei within the framework of DF model generally needed normalization to obtain satisfied agreement results with the experimental data.

Thus, we used the case two potential parameters in the inelastic scattering analysis. The difficulty in fitting elastic scattering cross sections is reflected in the inelastic predictions and indicated a deficiency in the present potential form.

The analysis of the inelastic scattering of the ${}^3\text{He}$ particles has been performed and the comparison of theoretical calculations and the experimental data has been presented in Fig. 2.

Table 2. Real normalization factor and χ_R^2 values from best fit to inelastic scattering data for different levels of ${}^{90}\text{Zr}$, ${}^{116}\text{Sn}$ and ${}^{208}\text{Pb}$.

reaction	n	level	N_{rr}	χ_R^2
${}^3\text{He}+{}^{90}\text{Zr}$	2	2.18(2^+)	0.13	0.14
		2.75(3^-)	1.40	0.14
${}^3\text{He}+{}^{116}\text{Sn}$	2	1.29(2^+)	0.17	0.03
		2.27(3^-)	0.84	0.03
${}^3\text{He}+{}^{208}\text{Pb}$	2	4.09(2^+)	0.23	0.19
		2.61(3^-)	1.44	0.16

In the case of ${}^{90}\text{Zr}$ and ${}^{208}\text{Pb}$ (3^-) state, there is an overestimation in forward regions and poor agreement in case ${}^{208}\text{Pb}$ (2^+) state. The potentials for elastic scattering analysis are subsequently used to calculate the inelastic scattering cross sections. The calculations are performed using the modified DWUCK4. The inelastic potentials are calculated according to the following form

$$U^\lambda(r) = N_{\text{rr}} V^\lambda(r) + iW^\lambda(r), \quad (9)$$

where λ is the multi-polarity [19]. $V^\lambda(r)$ is the real folded (transition) inelastic potential multiplied by the normalization factor N_{rr} and $W^\lambda(r)$ is an imaginary deformed PWS potential. The calculated real folded inelastic potential normalization factor N_{rr} as well as the corresponding values of χ_R^2 are shown in Table 2.

3 Conclusion

Although there are many detailed analyses concerning the elastic and inelastic scattering angular distributions of these investigated systems studied in OM with various potential forms, just a few of them make an effort to evolve a systematization for the folding potential parameters. So, we have re-analyzed elastic and inelastic scattering of ^3He particles with ^{90}Zr , ^{116}Sn and ^{208}Pb at 270 MeV with minimal 4-parameter nuclear potential sets having (WS^2+iPWS^2) and $(WS+iPWS)$ forms. When the real potential parameters are used with different normalization factors given in this work, FM analyses with these two folded potential sets have provided

different results. Calculations with the squared potential forms can reproduce the experimental elastic angular distributions in a good agreement, especially in case ^{116}Sn . The difficulty found in fitting elastic scattering cross sections is reflected in the inelastic predictions in case ^{90}Zr and ^{208}Pb and indicated a deficiency in the present potential form.

However, this approach has shown that an increase of power (n) from 1 to 2 is accompanied by an increase of real normalization factor ($N_r=1$ for all cases) values, i.e. it does not need normalization to fit the data. The similarities and differences between the two cases used in our analysis are pleasantly visible in this comparison. Generally on the basis of these results, we conclude that the WS^2 form is more suitable than the PWS form for real potential.

The author thanks researcher Ahmed Fouad (Faculty of Education, Physics and Chemistry department, Alexandria University, Egypt) for providing an additional form factor form WS^2 in the DWUCK4 program.

References

- 1 Satchler G R. Direct Nuclear Reactions. Oxford: Clarendon Press, 1983. 392
- 2 Singh P P, LI Q, Schwandt P, Jacobs W W, Saber M, Stephenson E J, Saxen A, Kailas S. Pramana J. Phys., 1986, **27**(6): 747
- 3 Yamagata T, Utsunomiya H, Tanaka M, Nakayama S, Koori N, Tamii A, Fujita Y, Katori K, Minoue, Fujiwara M, Ogata H. Nucl. Phys. A, 1995, **589**: 425
- 4 Sakuragi Y, Katsuma M. Nucl. Instrum. Methods Phys. Res. A, 1998, **402**: 347
- 5 Satchler G R. Introduction to Nuclear Reactions. London: Mc Millan Press Ltd., 1980. 153
- 6 Krane K S. Introductory Nuclear Physics, New York: John Wiley and Sons, 1988. 396
- 7 Brandan M E, Satchler G R. Phys. Rep., 1997, **285**: 143
- 8 El-Hammamy M N, Attia A, El-Akkad F A, Abdel-Moneim A M. Chin. Phys. C, 2014, **38**(3): 034102
- 9 Cook J. Comput. Phys. Comm., 1982, **25**: 125
- 10 Satchler G R, Love W G. Phys. Rep., 1979, **55**: 183
- 11 El-Azab Farid M, Mahmoud Z M M, Hassan G S. Nucl. Phys. A, 2001, **691**: 671
- 12 Azab Farid M El, Mahmoud Z M M, Hassan G S. Phys. Rev. C, 2001, **64**: 014310
- 13 Chwieroth F S, TANG Y C, Thompson D R. Phys. Rev. C, 1974, **9**: 56
- 14 El-Azab Farid M, Hassanain M A. Nucl. Phys. A, 2000, **678**: 39
- 15 DeJager C W, DeVries H, DeVries C. Atomic Data and Nuclear Data Tables, 1974, **14**: 479
- 16 Kunz P D. University of Colorado (unpublished)
- 17 Kürkçüoğlu M E, Aytakin H, Boztosun I. Modern Physics Letters A, 2010, **21**(29): 2217
- 18 Budzanowski A, Alderliesten C, Bojowald J, Oelert W, Turek P, Dabrowski H, Wiktor S. Proceedings of the Karlsruhe International Discussion Meeting 1979. 219
- 19 Khoa D T, Satchler G R. Nucl. Phys. A, 2000, **668**: 3–41